7th Int. Symp. "Nanostructures: Physics and Technology"
St Petersburg, Russia, June 14–18, 1999

Temperature dependence of spontaneous emission and threshold characteristics for 1.3 μm InGaAs/GaAs quantum dot GaAs-based lasers

D. L. Huffaker, O. Shchekin, G. Park, Z. Z. Zou, S. Csutak and D. G. Deppe
Microelectronics Research Center, The University of Texas at Austin
10100 Burnet Rd., Bldg. 160, M.S. R9900 Austin, TX 78758, USA

Quantum dot (QD) active regions are rapidly advancing for use in semiconductor lasers [1–2]. The atomic-like density of states promises several improvements in laser diode performance including ultralow threshold current density and temperature insensitive threshold. Another important characteristic is the possibility for extended wavelength ($\lambda > 1.1\ \mu$m) emission from GaAs-based devices [3–5]. This has been demonstrated in a QD vertical cavity surface emitting laser that emits at 1.15 μm [6], a resonant cavity QD photodetector operating at 1.27 μm [7] and more recently in edge-emitting lasers that use low loss cavities and operate at the wavelength of 1.31 μm at room temperature [8].

Here, we present data characterizing the temperature dependence of spontaneous emission and lasing characteristics for 1.3 μm InGaAs/GaAs quantum dot (QD) GaAs-based lasers. While efficient ground state emission is achieved at 80 K, the spontaneous efficiency decreases with increasing temperatures. Similarly, ultralow threshold current density (20 A/cm^2) is obtained at 77 K. Although the lasing threshold remains temperature insensitive to 200 K, it increases rapidly at higher temperatures. With high reflectivity coated facets, room temperature threshold current densities as low as 90 A/cm^2 are achieved. We have modeled these device characteristics as a function of temperature. From our analysis, we attribute these temperature characteristics to an increased nonradiative recombination rate from the QD higher energy levels and wetting layer. Our results suggest that very low threshold current density can be obtained at room temperature once nonradiative recombination is eliminated.

The QD active region is grown by molecular beam epitaxy in a GaAs barrier region surrounded by a $Al_{0.20}Ga_{0.80}As$ average composition waveguide region and a $Al_{0.70}Ga_{0.30}As$ cladding region. The InGaAs QDs are formed from a total of 11 monolayers of In, Ga and As deposited by sub-monolayer depositions [5]. A QD density of 10^{10} dots/cm^2 is measured using atomic force microscopy. Broad-area edge-emitters are fabricated. Devices with very short cavity length ($L < 1.0$ mm), in which lasing is inhibited due to edge loss, have been studied in spontaneous emission. Longer cavities are studied as lasers both with and without high reflectivity (HR) coated facets.

The electroluminescence output power is measured versus current and converted to efficiency versus current density. The results are shown in Fig. 1. At 80 K, the peak efficiency is 0.5% at 5 A/cm^2 which corresponds to ground state emission. We believe this represents close to 100% internal quantum efficiency. With increased current density and subsequent increased level filling the efficiency drops to 0.20% at 100 A/cm^2. This indicates that an increased nonradiative recombination rate exists for the higher energy levels even at low temperatures. At 160 K, the peak efficiency drops to 0.34% at 5 A/cm^2. At 250 K and 300 K, the peak efficiencies are 0.11% and 0.04% at current densities of 10 A/cm^2 and 40 A/cm^2, respectively. This indicates that temperature dependent nonradiative recombination is present in the QDs. Furthermore, we see that the radiative efficiencies vary for samples which are grown under similar conditions. Room temperature electrolumines-

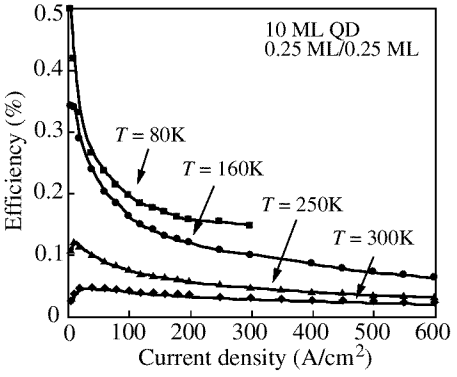

Fig. 1. Spontaneous efficiency versus current density measured for several temperatures. Two trends are observed. The ground state efficiency decreases with increasing temperature, and the efficiency at each temperature decreases with increasing current density.

cence efficiencies as high as 0.20% have been measured [5]. Therefore, we attribute the nonradiative recombination to point defects on the QD surface or within the QD bulk [9].

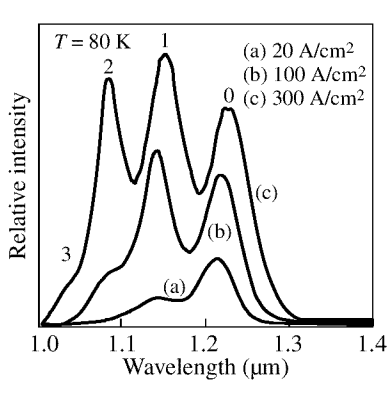

Fig. 2. Spontaneous emission spectra at 80 K for three different current densities.

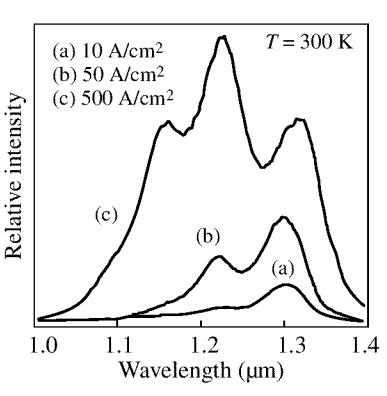

Fig. 3. Spontaneous emission spectra at 300 K for three different current densities.

To evaluate level filling, we measured spontaneous emission spectra for different current densities and different temperatures. Figure 2 shows spontaneous emission spectra at three different current densities for $T = 80$ K. At 5 A/cm^2 (spectra not shown) only the ground state is excited with a 40 meV linewidth centered at 1.22 μm. With increasing current to 20 A/cm^2, the first excited state, at 1.14 μm is partially filled. At 100 A/cm^2 and 200 A/cm^2, the second and third excited states at 1.09 μm and 1.04 μm, respectively, are filled. At 300 K, the spectra has similar behavior. Figure 3 shows 300 K spontaneous spectra from the same device measured at 10 A/cm^2, 50 A/cm^2 and 500 A/cm^2. The ground state emission peak occurs at 1.31 μm with a 40 meV linewidth. We observe that higher current densities are necessary to achieve bandfilling, which is consistent with a reduced electroluminescence efficiency. At both 80 K and 300 K, the higher energy levels begin to fill before the ground state saturates.

Figure 4 shows light versus current curves and spectra measured under room-temperature pulsed conditions for a QD laser ($L = 2.76$ mm) with high reflectivity (HR) coated facets. These lasers are made from the same epitaxial wafer as the shorter devices characterized in

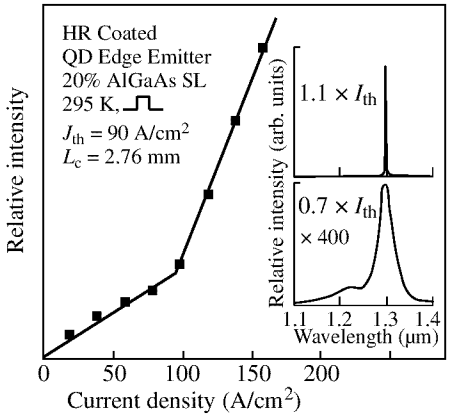

Fig. 4. Light versus current and spectral data taken at 300 K under pulsed operation. The laser is 2.76 mm long with HR-coated facets. The threshold is 90 A/cm^2 and the lasing wavelength is 1.31 μm.

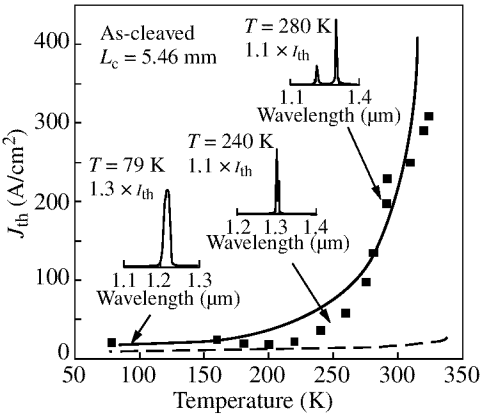

Fig. 5. Threshold current density versus temperature for a 5.46 mm long cavity with as-cleaved facets. Lasing occurs on the ground state for temperatures from 79 K to 280 K and on the first excited state for temperatures higher than 280 K. The solid curve shows calculated threshold current density versus temperature. The dashed curve shows calculated threshold current density if the nonradiative recombination rate is zero.

Figs. 1–3. A low threshold current density of 90 A/cm^2 is achieved at the 1.31 μm lasing wavelength. With HR coatings, this laser will operate from the ground state throughout the range of operation (up to 325 K). The upper limit of the temperature range is set by the dewar.

The temperature dependence of threshold from 77 K to 324 K for a longer cavity (L = 5.46 mm) with as-cleaved facets, also from the same wafer, is shown in Fig. 5. Spectral data at three different temperatures are shown as insets. At 79 K the threshold current density is 20 A/cm^2. From T = 79 K up to T = 200 K the threshold is nearly independent of temperature. Within this range, the carriers occupy the ground states of dots where the nonradiative recombination rate is low. At temperatures higher than 220 K, the threshold increases quickly due to increased carrier occupation of the higher energy levels and the wetting layer which causes increased nonradiative recombination. The spectral insets show that lasing occurs on the ground state within the temperature range of 79 K to 280 K and on the first excited state for higher temperatures. At 79 K, the carriers are confined to individual QDs with a low probability of escape relative to the radiative recombination. The lasing spectrum is therefore multimode and broad due to spectral hole burning [10]. At 240 K, the spectrum shows a decreased number of lasing modes due to thermal coupling of the QD ensemble through the wetting layer [11]. At 280 K, the spectrum shows both the ground state and the first excited state lasing simultaneously. Above 280 K, the laser operates from the first excited state.

We have performed extensive modeling of the temperature characteristics for 1.3 μm QD lasers based on a 2D harmonic oscillator density of states [9]. The model accounts for carrier scattering and radiative and non-radiative recombination between the QD energy levels. Material parameters such as non-radiative and radiative recombination rates and scattering rates are determined by fitting calculated data to experimental data. In order to

limit the number of adjustable parameters, we have assumed symmetrical electron and hole levels and scattering rates. Despite the assumption, we can achieve reasonable agreement with experimental data such as electroluminescence efficiencies, spontaneous spectra and threshold current densities. In Fig. 5, we show the calculated threshold current density overlaid on the experimental data points. The solid curve shows the calculated threshold current density using a nonradiative recombination rate that is consistent with our experimental data. The dashed curve shows the calculated threshold current density assuming that the nonradiative recombination rate equals zero. The model indicates that the increase in threshold with increasing temperature is due to an increasing population of higher energy levels and that carriers in higher energy levels have a higher nonradiative recombination rate due to an increased number of nonradiative recombination paths compared to radiative recombination paths. Our results therefore predict quite low threshold current density at room temperature if nonradiative recombination is eliminated from the QDs. We will discuss the model and calculated parameters as well as QD crystal growth in more detail during the presentation.

Acknowledgments

This work has been supported by the National Science Foundation and the State of Texas Advanced Research Program.

References

[1] N. Kirstaedter, N. N. Ledentsov, M. Grundmann, D. Bimberg, V. M. Ustinov, S. S. Ruvimov, M. V. Maximov, P. S. Kop'ev, Zh. I. Alferov, U. Richter, P. Werner, U. Gosele and J. Heydenreich, *Electron. Lett.* **30**, 1416 (1994).

[2] H. Shoji, K. Mukai, N. Ohtsuka, M. Sugawara, T. Uchida and H. Ischikawa, *IEEE Phot. Tech. Lett.* **7**, 1385 (1995).

[3] K. Mukai, O. Nobuyuki, S. Mitsuru and S. Yamzaki, *Jpn. J. Appl. Phys.* **33**, L1710 (1994).

[4] R. Mirin, J. Ibbetson, K. Nishi, A. Gossard and J. Bowers, *Appl. Phys. Lett.* **67**, 3795 (1995).

[5] D. L. Huffaker and D. G. Deppe, *Appl. Phys. Lett.* **73**, (1998).

[6] D. L. Huffaker, H. Deng and D. G. Deppe, *IEEE Phot. Tech. Lett.* **10**, 185 (1998).

[7] J. C. Campbell, D. L. Huffaker, H. Deng and D. G. Deppe, *Electron. Lett.* **33**, 1337 (1997).

[8] D. L. Huffaker, G. Park, Z. Zou, O. Shchekin and D. G. Deppe, *Appl. Phys. Lett.* **73**, (1998).

[9] D. G. Deppe, D. L. Huffaker, S. Csutak, Z. Zou, G. Park and O. B. Shchekin, *submitted to IEEE J. Quantum Elect.*

[10] G. Park, D. L. Huffaker, Z. Zou, O. B. Shchekin and D. G. Deppe, *IEEE Phot. Techn. Lett.* **11**, (1999) (accepted for publication).

[11] A. E. Zhukov, V. M. Ustinov, A. Y. Egorov, A. R. Kovsh, A. F. Tsatsulnikov, N. N. Ledentsov, S. V. Zaitsev, N. Y. Gordeev, P. S. Kopev and Zh. I. Alferov, *Jap. J. Appl. Phys.* **37**, 4216 (1997).